Basins of attraction for cascading maps

Erik Boczko

Department of Biomedical Informatics

Vanderbilt University

Nashville, TN 37232

615-936-6668

erik.m.boczko@vanderbilt.edu

Todd Young

Department of Mathematics

Ohio University

Athens, OH 45701

740-593-1285

young@math.ohiou.edu

February 1, 2008

Abstract

We study a finite uni-directional array of "cascading" or "threshold coupled" chaotic maps. We describe some of the attractors for such systems and prove general results about their basins of attraction. In particular, we show that the basins of attraction have infinitely many path components. We show that these components always accumulate at the corners of the domain of the system. For all threshold parameters above a certain value, we show that they accumulate at a Cantor set in the interior of the domain. For certain ranges of the threshold, we prove that the system has many attractors.

1 Cascading maps and applications

Let $f(x) = 4x(1-x)$. Let $c_1 \in (0,1)$ and call it a *threshold*. Formally, we define a *cascading*, or, *threshold coupled* system of N maps as a dynamical system on $[0,1]^N$ represented by a function $F_{c_1} : [0,1]^N \to [0,1]^N \times \mathbb{R}$, that consists of iteration at each site by f, followed by "cascading", i.e.,

$$F_{c_1} = \mathcal{C} \circ (f \times \cdots \times f),$$

where $\mathcal{C}$ is a cascading operator. Specifically,

$$f \times \cdots \times f : ((x_1^j, \ldots, x_N^j)) \mapsto (y_1^j, \ldots, y_N^j) = (f(x_1^j), \ldots, f(x_N^j))$$

1

is simultaneous, independent iteration by f at each site and

$$\mathcal{C} : [0,1]^N \to [0,1]^N \times \mathbb{R}$$
$$: (y_1^j, \ldots, y_N^j) \mapsto (x_1^{j+1}, \ldots, x_N^{j+1}, e^{j+1}). \tag{1}$$

The map F_{c_1} produces both the new state $(x_1^{j+1}, \ldots, x_N^{j+1})$ as well as an *excess* e^{j+1}. The cascade map $\mathcal{C}$ acts on $(y_1^j, \ldots, y_N^j)$ sequentially from left to right in the following fashion. If $y_1^j \le c_1$, then let $x_1^{j+1} = y_1^j$ and define $e_1^j = 0$. If however, $y_1^j \ge c_1$, then let $x_1^{j+1} = c_1$ and define $e_1^j = y_1^j - c_1$. Next we consider the second site in the array in the same way except we first add the value of e_1^j to y_2^j. That is, if $\hat{y}_2^j = y_2^j + e_1^j \le c_1$, then let $x_2^{j+1} = \hat{y}_2^j$ and let $e_2^j = 0$. Otherwise, let $x_2^{j+1} = c_1$ and define $e_2^j = \hat{y}_1^j - c_1$. The value of e_2^j is cascaded forward to the third site and this pattern continues to the end of the array. The final excess e_N^j is the e^{j+1} that appears in (1). It is "removed" from the system and the sequence $\{e^j\}$ is considered as the "output".

In applications, c_1 has been used as a tunable parameter and $\{e^j\}$ has been used as a time-series that characterizes the dynamics of the system. Cascading maps have been considered for use in chaos-based computation [SinDit99] and for classification of gene expression data [Par02]. In these potential applications initial conditions are classified based on the eventual output $\{e^j\}$, which depends on the attractor into which the orbit falls. Thus it is important to have a clearer understanding of the attractors and their basins of attraction. An attractive aspect of cascading systems is that they can be applied using a single tunable parameter. Cascading dynamics of continuous time oscillators has also been considered [Kap76] and its use in communications has been explored [KMS99].

We will study attractors for F and the associated basins, i.e. the set of initial conditions which approach the attractors. In numerical studies it appears that these basins are usually quite complicated. We prove that under some conditions, the basins of attraction have infinitely many components. Our main result Theorem 3.7 shows that the components of the basins accumulate at a Cantor set in the interior of the domain. That is, for each point in the Cantor set, every neighborhood of the point intersects infinitely many components of the basins. By component of a set, we mean connected component. In $\mathbb{R}^N$ connectedness is the same as path connectedness, i.e. any two points in a component can be connected by a continuous curve. We also show the existence of at least two types of periodic attractors, and that there are large ranges of threshold values for which there many attractors.

For convenience we also define the related *threshold map* as a map $f_{c_1} : [0,1] \rightarrow [0,1] \times \mathbb{R}$ by

$$f_{c_1}(x) = \begin{cases} f(x), & \text{if } f(x) < c_1 \\ c_1, & \text{if } f(x) \geq c_1, \end{cases}$$

and we will denote the *excess* $f(x) - c_1$ for f_{c_1} by $e(x)$.

2 Dynamics of a single threshold map

It is well known that $f = 4x(1-x)$ is topologically conjugate to the tent map. (See for instance [ASY97, p. 114].) We will rely heavily on this fact in the proofs. Note that this method is not restrictive, but is quite general since any unimodal map f with topological entropy $h_{top}(f)$ is semi-conjugate to a tent map with slope $s = \exp(h_{top}(f))$ [MilThu88]. In cases where f is smooth and chaotic in the sense of having an absolutely continuous invariant measure, this semi-conjugacy is in fact a conjugacy and smooth at almost all points. Also note that any orbit of f that is bounded away from the critical point is uniformly hyperbolic (repelling). To see this, consider the metric provided by the conjugacy with the tent map. In that metric the uniform expansion rate is 2. Finally, note that orbits of f_{c_1} that stay below the threshold inherit these properties. For general maps f under some restrictions, if an orbit is bounded away from a critical point then it is hyperbolic (see Theorem III.5.1 in [MelStr93]).

Let C be the set of x such that $f(x) \geq c_1$. One easily finds that

$$C = [c_0, 1 - c_0] = \left[\frac{1}{2} - \frac{1}{2}\sqrt{1 - c_1}, \frac{1}{2} + \frac{1}{2}\sqrt{1 - c_1} \right].$$

Thus $f_{c_1}(C) = \{c_1\}$ and $f_{c_1}^{-1}(c_1) = C$. Denote the forward orbit of c_1 by c_2, c_3, ...

For $c_1 < 3/4$, it is easily seen that f_{c_1} has a single attracting periodic point. We will restrict our attention to $c_1 > 3/4$. The following proposition is elementary.

Proposition 2.1 *For $c_1 > 3/4$, f_{c_1} has an absorbing set $A = [c_2, c_1]$ and all points, except 0 and 1, are eventually mapped into A.*

Given a periodic orbit, the set of all points that have backward orbits which are asymptotic to the orbit of x we call the *unstable manifold* of the periodic orbit.
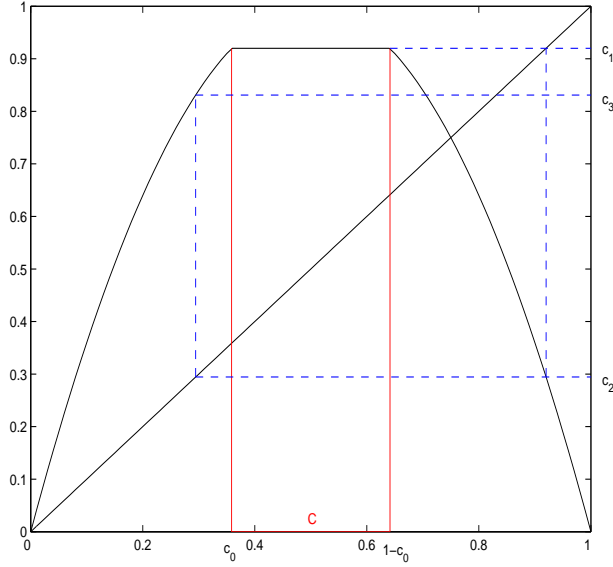
Figure 1: Three iterations of the threshold map $f_{0.92}$. The interval $C = [c_0, 1 - c_0]$ is the set on which $f_{c_1}(x) = c_1$. Almost all orbits eventually enter C. The interval $A = [c_2, c_1]$ absorbs all points except 0 and 1.

Proposition 2.2 *For $c_1 > 3/4$, the unstable manifold of the fixed point at $3/4$ is A. Given any point a in A, there is a sequence of points $\{a_{-j}\}_{j=1}^{\infty}$ that converges to $3/4$ and such that $f_{c_1}^j(a_{-j}) = a$. Further, a_{-j} can be chosen so that $\{a_{-i}\}_{i=1}^j$ does not intersect C.*

Proof: For $c_1 > 3/4$ it is easily seen that $f([1 - c_0, c_1]) = A$ and that $[1 - c_0, c_1]$ is in the unstable manifold of $3/4$. Since a has a preimage in $[1 - c_0, c_1]$ and since f is invertible on $[1 - c_0, c_1]$ all preimages of a exist in this interval. Since $(1 - c_0, c_1]$ is mapped onto all of A except for c_1 iterates of a_{-j} may avoid C. $\qquad\square$

Proposition 2.3 *For $c_1 > 3/4$, the unstable manifold of the fixed point at 0 is $[0, c_1]$. Given any point a in A, there is an integer j_0 and a sequence of points $\{a_{-j}\}_{j=j_0}^{\infty}$ that converges to 0 such that $f_{c_1}^j(a_{-j}) = a$.*

Proof: Note that $[0, c_0]$ is in the unstable manifold of 0 and that its image is $[0, c_1]$. The proof is then as for the previous proposition. $\qquad\square$

Outside of A the only invariant set is the fixed point at 0.

4

Inside A we may have two types of invariant sets, a super-stable or semi-stable periodic orbit, and a hyperbolic repelling set Λ in $A \backslash C$. By super-stable we mean that the multiplier of the periodic orbit is 0, i.e. the orbit passes through the interior of C. A semi-stable orbit occurs at threshold values for which a periodic orbit intersects the boundary of C. Because of the hyperbolicity outside C, there are only two possibilities for the forward orbit of c_1; it lands in C or it lands on Λ.

It follows from properties of f that any hyperbolic repelling set Λ must have measure zero and any super-stable orbit must attract Lebesgue almost all other points. Both of these conclusions follow from the fact that the forward orbit of Lebesgue almost every point must intersect C. This follows easily for the case $f = 4x(1-x)$ by the conjugation with the tent map. For more general maps see Theorem 2.2 in [HomYou02].

The dynamics of the threshold map is very simple for $\frac{3}{4} < c_1 < \frac{5+\sqrt{5}}{8} \approx 0.904508497$ as described by the next result.

Proposition 2.4 *For*

$$\frac{3}{4} < c_1 < \frac{5+\sqrt{5}}{8}$$

f_{c_1} *has a super-stable period 2 orbit and* $\Lambda = \{3/4\}$.

Proof: One can easily solve $f(c_1) \in C$ to obtain the limits of the above inequality. For such threshold values $c_2 > c_0$, so $A \setminus C = [1 - c_0, c_1]$. All points in this interval except $\{3/4\}$ eventually leave the interval and must then enter C. $\qquad\square$

From numerical studies such as in [Sin94] it is apparent that the bifurcations become complex after $c_1 = \frac{5+\sqrt{5}}{8}$. These bifurcations accumulate at the value $c_1 = \xi_2 \equiv \frac{2+\sqrt{3}}{4} \approx 0.933012702$, which is the location of the second "star" in the bifurcation diagram as described in [Sin94]. In fact we have:

Proposition 2.5 *There exists a sequence of open intervals* $\{J_k\}_{k=2}^{\infty}$ *that accumulates at* ξ_2, *such that for* $c_1 \in J_k$, *the map has a super-stable periodic orbit of period* k. *For* k *even,* J_k *is to the left of* ξ_2 *and* J_k *is to the right of* ξ_2 *when* k *odd.*

Proof: The parameter value ξ_2 is a solution of
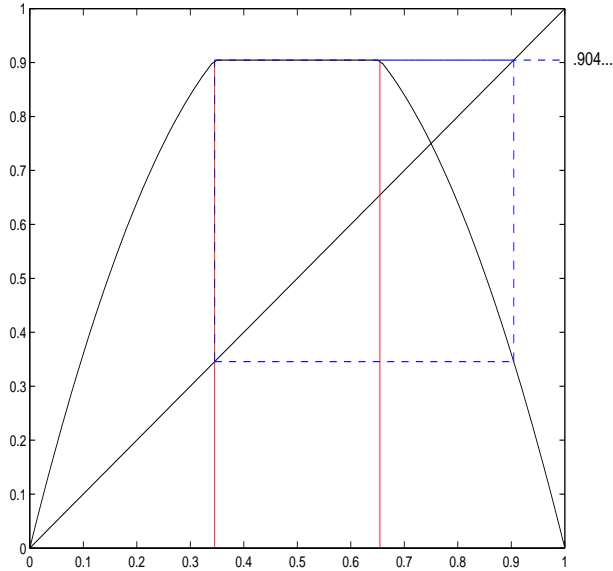
$$f^2(\xi_2) = \frac{3}{4}.$$

5

Figure 2: For $c_1 = \frac{5+\sqrt{5}}{8} \approx .904508497$, f_{c_1} maps c_1 onto c_0. For all c_1 in $(3/4, \frac{5+\sqrt{5}}{8})$, the threshold value c_1 is a super-stable period 2 point.

That is, the threshold value is mapped exactly onto the unstable fixed point at $3/4$. Note that there exist a sequence of inverse images of C that accumulate on both sides of $3/4$. These inverse images vary smoothly with respect to c_1. Further note that as c_1 passes from $\frac{5+\sqrt{5}}{8}$ to 1, $f^2(c_1)$ passes from $1 - c_0$ to 1, Thus as c_1 is varied, $f^2(c_1)$ must pass through all of the inverse images of C surrounding $3/4$. As it does the super-stable orbits occur. $\square$

Sinha [Sin94] showed that there also exist threshold values ξ_s, $s > 2$, approaching 1 for which

$$f^s_{\xi_s}(\xi_s) = \frac{3}{4}$$

and $f^i_{\xi_s}(\xi_s) < \frac{1}{2}$, for all $1 \le i \le s - 1$. Further, he showed that these values satisfy

$$\lim_{s \to \infty} \frac{\xi_{s+1} - \xi_s}{\xi_s - \xi_{s-1}} = \frac{1}{4}.$$

These parameter values correspond to "stars" in the bifurcation diagram. They can be understood as highly degenerate homoclinic bifurcations. For each such parameter, the repelling fixed point at $3/4$ has an interval of homoclinic orbits. Each of these threshold values has bifurcation structures similar to those in Proposition 2.5

Let $\{b_{2k}\}$ be the right endpoints of the even-index intervals $\{J_{2k}\}$.
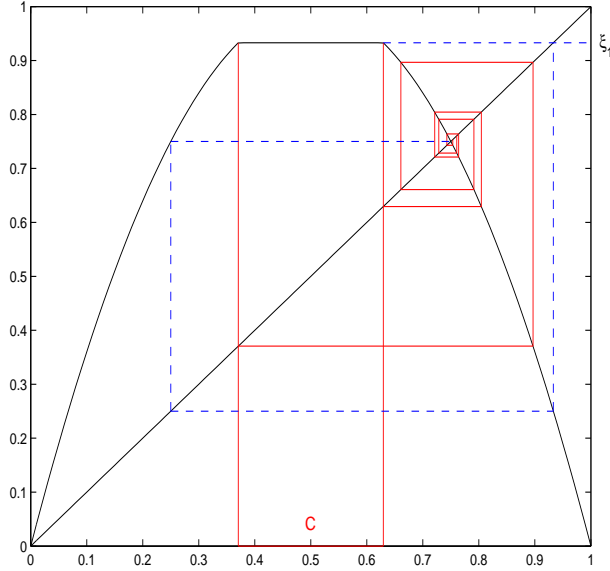
Figure 3: The threshold map f_{ξ_2} maps C onto the unstable fixed point at $3/4$ in three iterations. Also, inverse images of C accumulate at $3/4$.

Proposition 2.6 *For each b_{2k}, the map $f_{b_{2k}}$ has a semi-stable period $2k$ orbit. This orbit persists and is repelling for all $c_1 > b_{2k}$.*

Proof: For b_{2k}, the right endpoint $1 - c_0$ of C is $2k$ periodic. This periodic orbit is a periodic orbit of f that intersects C only at $1 - c_0$. For higher threshold values C is strictly smaller, so it does not intersect the periodic orbit. Thus the periodic orbit persists for larger c_1. It is hyperbolic repelling since it does not intersect C. $\qquad\qquad\square$

Thus the hyperbolic attractor Λ becomes increasingly complex as c_1 moves from $\frac{5+\sqrt{5}}{8}$ to $\xi_2 \equiv \frac{2+\sqrt{3}}{4}$. At ξ_2 it becomes truly complex and the underlying dynamics become chaotic.

Theorem 2.7 *For $c_1 > \xi_2$, f_{c_1} has positive topological entropy and Λ is uncountable. Further, f restricted to Λ is transitive, i.e. there is a heteroclinic orbit between any two periodic points.*

Proof: For $c_1 < \xi_2$, $f_{c_1}((c_2, c_0))$ contains $3/4$, and at the same time $(c_2, c_0) \subset A = W^u(3/4)$. In particular, there exists a sequence of intervals $\{J_{-i}\}$, $i = 1, 2, \ldots$, that are in the inverse image of $J_0 = (c_2, c_0)$ that converge to $3/4$ as $i \to \infty$. Thus, for all $i \leq -n_0$, we have that

7

$J_{-i} \subset f_{c_1}(c_2, c_0)$. The collection $\{J_{-i}\}_0^\infty$ forms a Markov partition (see [KatHas95]). If we consider a finite number of these intervals, $\{J_{-i}\}_0^n$, with $n \geq n_0 + 1$ then the transition matrix for this partition has zeros everywhere except for the ones on super-diagonal and ones in the last $n - n_0 + 1$ entries in the first column.

$$
M_n = \begin{pmatrix}
0 & 1 & 0 & 0 & 0 & \cdots & 0 \\
0 & 0 & 1 & 0 & 0 & \cdots & 0 \\
\vdots & 0 & 0 & \ddots & 0 & \cdots & 0 \\
0 & \vdots & \ddots & \ddots & \ddots & \ddots & \vdots \\
1 & \vdots & \cdots & \cdots & 0 & 1 & 0 \\
\vdots & \vdots & \cdots & \cdots & 0 & 0 & 1 \\
1 & 0 & \cdots & \cdots & 0 & 0 & 0
\end{pmatrix}.
$$

These matrices have an eigenvalue greater than 1, so we have that there is an invariant set Λ_n in $\{J_{-i}\}_0^n$ on which f_{c_1} is semi-conjugate to the Markov shift defined by M_n (see Theorem 15.1.5 in [KatHas95]). Hyperbolicity implies the semi-conjugacy is a conjugacy. In particular Λ_n is uncountable and f_{c_1} restricted to it has positive topological entropy and is transitive. Since Λ_n is invariant, it is contained in Λ. Further, $\Lambda = \left(\bigcup_{n=n_0}^\infty \Lambda_n \right) \bigcup \{3/4\}$ since a point in Λ other than $3/4$ must enter J_0, every point in Λ must be contained J_0 or one of the inverse images of J_0. Since f is transitive on each Λ_n, it is transitive on Λ which is the closure of the union of the set Λ_n. $\qquad\square$

The following is an easy consequence of Proposition 2.2

Proposition 2.8 *For $c_1 > \xi_2$, the unstable manifold of any periodic point in Λ is A.*

Finally, we show that a super-stable orbit almost always occurs.

Proposition 2.9 *For almost all c_1, f_{c_1} has a super-stable orbit.*

Proof: Using the conjugacy with the tent map, one easily sees that the inverse images of C form a full-measure subset of $[0, 1]$. Its complement, which is the invariant set Λ, must have measure zero. Let $\mathcal{C}$ denote the collection of all intervals J such that $f_{c_1}^k(J) = C$ and denote by $k(J)$, the minimal such integer k. If f_{c_1} does not have a super-stable orbit, then the orbit of c_1 must be disjoint from C, so its forward orbit must be in the invariant set Λ, i.e. it must land on the hyperbolic repelling set. This set has measure zero for all c_1 and

c_1	Attractor	Λ
.75 − .9045...	period 2	$\{3/4\}$
.9045... − .9330...	various	expanding
.9330... − 1.0	various	uncountable

Table 1: Summary of dynamics for a single threshold map.

points in the hyperbolic set do not depend on c_1, since they are inherited from f. On the other hand, the points c_k have a non-zero derivative with respect to c_1 as long as the orbit stays out of C. Thus for any k the set of c_1 for which c_k intersects the hyperbolic set has measure zero. Taking the union of these sets for all k we obtain a measure zero set. The compliment of this measure zero set is the set of c_1 which never land on the hyperbolic set and thus must have a super-stable orbit. $\qquad\square$

3   Consequences for cascading

Let F_{c_1} be a sequence of N threshold maps with cascading. If one were to consider N threshold maps without cascading, then the results of the last section would give a very detailed picture of the dynamics. Almost all initial conditions would fall into superstable periodic orbits at each site. These periodic orbits would exist at any phases relative to one another. Thus, there would be p^{N-1} distinguishable attractors. Basins of the attractors would be cross-products of the inverse images of C at each site, i.e. they would consist of rectangular boxes. One might then consider cascading as a (possibly not small) perturbation. We show in the next section that many features of the unperturbed system persist.

3.1   Absorbing sets and invariant sets

Proposition 3.1 *For $c_1 > 3/4$, F_{c_1} has an absorbing set $A^N = A \times \cdots \times A$ that attracts almost all orbits.*

Proof: For the threshold map f_{c_1}, A is an absorbing set that attracts almost all orbits, and thus almost any initial condition in the first site will reach A. For sites after the first, consider a value x_i^0 at the i-th site. If $x_i^0 < c_0$, then the dynamics, including the effects of

cascading only increase x_i, but cannot increase it past c_1. Since there are no fixed points in $[0, c_0]$ it will eventually enter $[c_0, c-1]$ and at least on the next iteration will be in A. If $x_i^0 > c_1$, then $x_i^1 < c_0$.

Once the orbit reaches A in any given map, cascading cannot remove it from A, since cascading can only increase the value at an individual map, but cannot increase it past c_1 which is the upper bound of A. $\qquad\qquad\qquad\qquad\qquad\qquad\qquad\qquad\qquad\qquad\qquad\square$

Proposition 3.2 *For $c_1 > 3/4$, the maximal hyperbolic repelling set of F_{c_1} in A^N is $\Lambda^N = \Lambda \times \cdots \times \Lambda$.*

Proof: Suppose that $x_i^j \in \Lambda$ for each i, Then the dynamics proceed at each site without cascading. On the other hand if $(x_1, \ldots, x_N)$ is in the maximal repelling set, then the forward orbit of x_i under f_{c_1} cannot leave $A \setminus C$. For the first site which is not subject to the effects of cascading, this implies that x_1 is in Λ. This implies that the first site will not have any excess, so the second site is not subject to cascading. Induction proves the result. $\square$

The next results follow from Proposition 3.2 and Propositions 2.4 and 2.7.

Corollary 3.3 *For $3/4 < c_1 < \frac{5+\sqrt{5}}{8} \approx .9045...$ the invariant set $\Lambda^N = \{3/4\}^N$.*

Corollary 3.4 *For $c_1 > \xi_2 \approx .9336...$ the invariant set Λ^N is uncountable.*

3.2 Structure of the basins

Theorem 3.5 *The basins of all attractors accumulate at the corners of $[0, 1]^N$. If a basin has a component contained in the interior of $[0, c_1]$ then every neighborhood of every corner of $[0, 1]^N$ contains infinitely many components of the basin.*

Proof: Let $(x_1^0, \ldots, x_N^0)$ be a point in the basin of an attractor. By Proposition 2.3, we can find a point $(x_1^{-j}, \ldots, x_N^{-j})$ near $(0, \ldots, 0)$ such that $f_{c_1}^j(x_i^{-j}) = x_i^0$ in such a way that the orbit is disjoint from C. Thus $(x_1^{-j}, \ldots, x_N^{-j})$ is mapped onto $(x_1^0, \ldots, x_N^0)$ by j j iterations of F. This shows that the basins accumulate at $(0, \ldots, 0)$. If a basin has a component in $[0, c_1]$, it must have a sequence of inverse images converging to $(0, \ldots, 0)$. Each of those inverse images must be components, otherwise the original component could be extended

10

along a continuous path. Since $f(1 - x) = f(x)$ this also implies the results at all the corners of $[0, 1]^N$. $\qquad\square$

Proposition 3.6 *For $c_1 > 3/4$ the unstable manifold of the fixed point $\{3/4\}^N$ is A^N.*

Proof: Let $a = (a_1, a_2, \ldots, a_N)$ a point in A^N. It follows from Proposition 2.8 that given any j there are points a_i^{-j} in $[1 - c_0, c_1]$ are mapped onto a_i by j iterations of f_{c_1}. Further, the first $j - 1$ iterates of a_i^{-j} do not intersect C, thus there is no cascading and the dynamics proceeds independently at each site. $\qquad\square$

Let $\tilde{\Lambda}$ be the transitive component of Λ containing $\{3/4\}^N$. That is a point $x \in \Lambda$ is in $\tilde{\Lambda}$ if and only any neighborhood of x contains points that are eventually mapped onto $\{3/4\}^N$.

Our main result is the following.

Theorem 3.7 *The basins of all attractors accumulate at each point in $\tilde{\Lambda}^N$. If a basin has a component contained in A^N, then each neighborhood of each point in $\tilde{\Lambda}^N$ contains infinitely many components. For $c_1 > \xi_2$, the above statements are true for Λ.*

Proof: It follows from Proposition 3.6 that given any point x in $\tilde{\Lambda}^N$ and any point a in A^N, there is a point arbitrarily close to y that is mapped into a. It then follows from the fact that F_{c_1} has a one to one inverse on $[1 - c_0, 1]^N$ that components accumulate at $\{3/4\}^N$. The rest of the conclusions follow from Propositions 2.7 and 3.6. $\qquad\square$

3.3   Examples of attractors

Proposition 3.8 *Suppose that for c_1, the threshold map, f_{c_1}, has a super-stable periodic orbit of period p. Then F_{c_1} has a super-stable periodic orbit of period p corresponding to in-phase synchronization of all N maps. The basin of attraction of this periodic orbit includes C^N and all its preimages.*

Proof: Suppose that the initial state $(x_1^0, x_2^0, \ldots, x_N^0)$ is contained in C^N. Then it is clear that one iteration of the system yields $(x_1^1, \ldots, x_N^1) = (c_1, \ldots, c_1)$ and an excess which is the sum of the excesses of each map. Since p is minimal $(x_1^j, x_2^j, \ldots, x_N^j) = (c_j, \ldots, c_j)$ for all $1 \leq j < p$ and $(x_1^p, \ldots, x_N^p) = (c_1, \ldots, c_1)$. The excess on step p will then be N times the

11

excess of each of the individual maps. Clearly the basin of attraction of the synchronized periodic orbit includes the preimages of C^N. □

The next result follows immediately from Propositions 2.9 and 3.8.

Corollary 3.9 *For almost all* c_1, F_{c_1} *has a super-stable periodic orbit.*

Next we consider another type of super-stable periodic orbit. We call a periodic orbit a *ripple* if $x_i^j = x_{i+1}^{j+1}$, for any $1 \le i \le N - 1$.

Proposition 3.10 *Suppose that* $c_1 > 15/16$ *and that* f_{c_1} *has a super-stable period* p *orbit. Then* F_{c_1} *has a super-stable, ripple periodic orbit. This orbit has a basin with a non-empty interior.*

Proof: Suppose the initial state $(x_1^0, \dots, x_N^0)$ is such that $x_1^0 \in C$, and

$$x_i^{i-1} < x_{i-1}^{i-2}$$

for each $2 \le i \le N$. Clearly we can find an open set of such initial conditions by taking x_i^0 in one of the i-th inverse images of (c_0, c_{p-1}). On the first step the excess from $f(x_1^0)$ is added to $f(x_2^0)$. The condition $c_1 > 15/16$ implies that $|f'(x)| < 1$ for all $x \in C$. This implies that x_i^{i-1} is in C, and thus $x_i^i = c_1$. □

For $N = 2$ and period $p = 2$ a ripple orbit might also be called an anti-phase periodic orbit. We can give a necessary and sufficient condition for the existence of such orbits.

Proposition 3.11 *Suppose that* f_{c_1} *has a super-stable period* 2 *orbit and* $N = 2$. *Then* F_{c_1} *has a super-stable anti-phase orbit if and only if*

$$c_2 + e(c_2) \le 1 - c_0. \tag{2}$$

The basin of this periodic orbit has a non-empty interior.

Proof: Consider the initial condition $(x_1^0, x_2^0) = (c_2, c_1)$. Since $f(c_1) = c_2$ and $f(c_2) = c_1 + e(c_2)$, we have that $(x_1^1, x_2^1) = (c_1, c_2 + e(c_2))$. It then follows that $(x_1^2, x_2^2) = (c_2, c_1)$. Thus the initial condition is part of a super-stable anti-phase orbit. It is clear that all initial conditions in a small open neighborhood of (c_2, c_1) will be mapped onto (c_2, c_1) by $F_{c_2}^2$.

Now suppose that the condition (2) is not satisfied. Any anti-phase orbit must contain the point $(x_1^j, x_2^j) = (c_2, c_1)$. However, if we apply the cascading map to (c_2, c_1) and $c_2 + e(c_2) > 1 - c_0$ then $x_1^{j+1} \neq c_1$, since $c_2 + e(c_2) \notin C$. $\qquad\square$.

For the only period two window $3/4 < c_1 < \frac{5+\sqrt{5}}{8}$, the equation in Proposition 3.11 is equivalent to:

$$19c_1 - 84c_1^2 + 128c_1^3 - 64c_1^4 < \frac{1 + \sqrt{1 - c_1}}{2}. \tag{3}$$

This can be solved symbolically. Using a numerical approximation the anti-phase orbit exists for

$$0.83627234814318\ldots < c_1 < \frac{5 + \sqrt{5}}{8} \approx .904508497. \tag{4}$$

Sinha and Ditto [SinDit99] considered the parameter value $c_1 \approx .84$ where both in-phase and anti-phase periodic orbit exist.

Finally, consider again the case of $N > 2$.

Theorem 3.12 *Suppose that $N > 2$ and c_1 is as in (4) or $c_1 > 15/16$ and f_{c_1} has a period p super-stable orbit.. Then there exist at least 2^{N-1} or p^{N-1} attractors, respectively.*

Proof: Since the dynamics at the first two sites is independent of the rest of the sites, both in-phase and anti-phase orbits exist in the first two sites. It follows from arguments above that in-phase and ripple synchronization of the third site with the second site exist. The rest are obtained by induction. $\qquad\square$.

4 Observations and conclusions

In Figures 4 - 9 we show basins of attractors of various threshold levels for a two site $(N = 2)$ cascading system. In these plots we have determined the basins of attractions for each point in a 499×499 grid. For each initial condition the system was allowed to evolve for 100 iterations in order to let it reach a steady state. Then the sum of the excesses were computed for the next 12 iterations. The plots shown are color representations of the resulting sum at each point in the grid. Blue indicates the lowest sum and red indicates the highest. Different colors must belong to different basins.

Let C^{-j} denote the j-th inverse image under f_{c_1} of C and let R_j denote the compliment of $\bigcup_{i=0}^{j} C^{-j}$ in $[0, 1]$, i.e. the set of points that avoid C for j steps. If we let m_T denote the

measure induced by the conjugacy with the tent map, then

$$m_T(R_j) = d_1^{j+1}$$

where d_1 is the value of the threshold in the tent map corresponding to c_1. It follows from Theorem 3.1 in [HomYou02] that

$$\frac{m(R_j)}{m_T(R_j)} \to 1$$

as $j \to \infty$, where m is Lebesgue measure. In other words, the asymptotic portion of points falling into C is the same with respect to Lebesgue measure as with respect to the induced measure. Explicitly, we have that the conjugacy takes c_1 to d_1 by:

$$d_1 = \frac{1}{\pi} \cos^{-1}(1 - 2c_1).$$

From this we may approximate $m(R_j)$ for various values of c_1 and j. For instance when $c_1 = .9$, we have $d_1 = .7952$ and so after 10 iterations 99% of all initial points fall into C. For $c_1 = .99$ it takes 35 iterations for the same percentage of points to fall into C. After 100 iterations, 99.9% of initial points fall into C when $c_1 = .99$. Thus, we expect that 100 iterations in our studies is sufficient for the system to reach steady state.

For $3/4 < c_1 < .83627...$ in-phase coupling is the only attractor. For $.83627... < c_1 < .90451...$ both in-phase and anti-phase period 2 attractors exists. In Figure 4 we show the basins for $c_1 = 0.84$. Basins are observed to accumulate at the corners of $[0,1]^2$.

At $c_1 = .904508497...$ a bifurcation occurs; for c_1 greater than this value the period 2 orbit ceases to exist. At the bifurcation (Figure 5) we notice that the boundary between basin is becoming non-smooth at some points.

In Figure 6 we find that the basins become complicated immediately past this bifurcation. However, from the numerics, is not yet fully complex. In contrast the accumulation of components of the basins appears to occur on a very complicated set, in Figure 7, for $c_1 = 0.93$ which is before ξ_2.

We find that the basins do not change radically at the bifurcation value ξ_2. In Figures 7-9 we show basins for various values of c_1. We observe that although the basins are quite complicated, they evolve is a very regular way.

Note that points in the basin component in the center of the graph correspond to in-phase locking. In all our experiments we see that this component includes C^2, but also
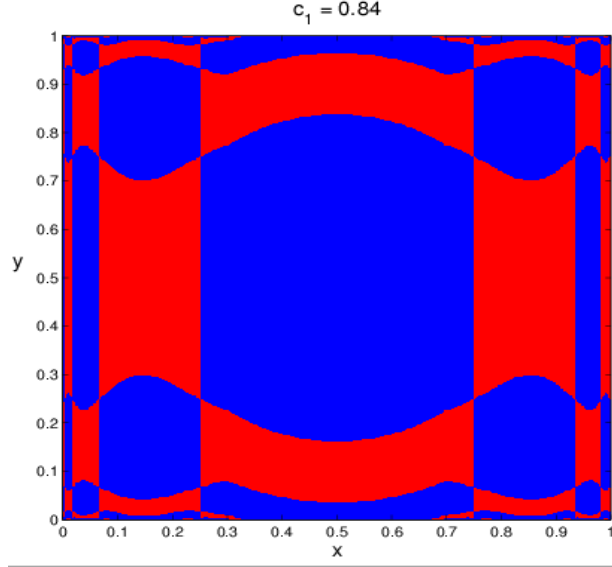
14

Figure 4: Basins of attraction for $N = 2$ and $c_1 = 0.84$. Here c_1 is in the range where both in-phase and anti-phase period 2 attractors exist.
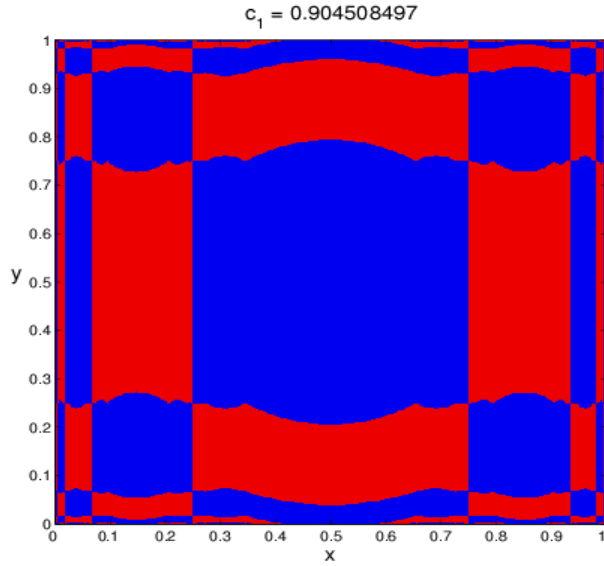

Figure 5: Basins of attraction for $N = 2$ and $c_1 = 0.904508497$. Here c_1 is at the upper end of the range for which period 2 attractors exist. Note that the boundaries of the basins appear to be non-smooth at some points.
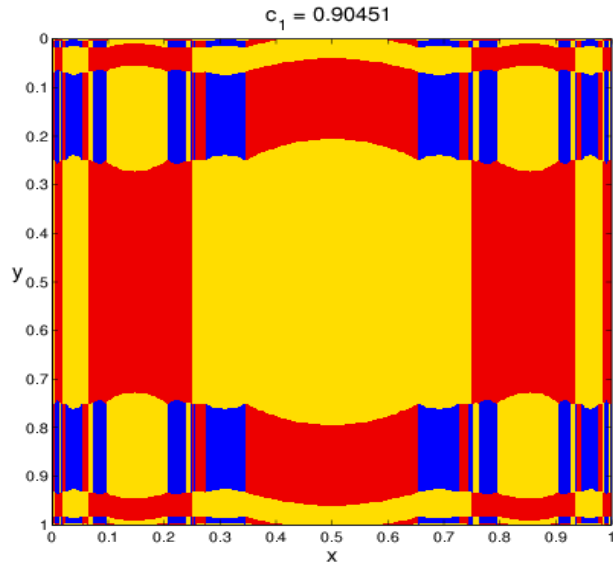
Figure 6: Basins of attraction for $N = 2$ and $c_1 = 0.90451$. This is just past the range for which period 2 attractors exist. Here we observe accumulation of components of the basins in the interior of $[0, 1]^2$.
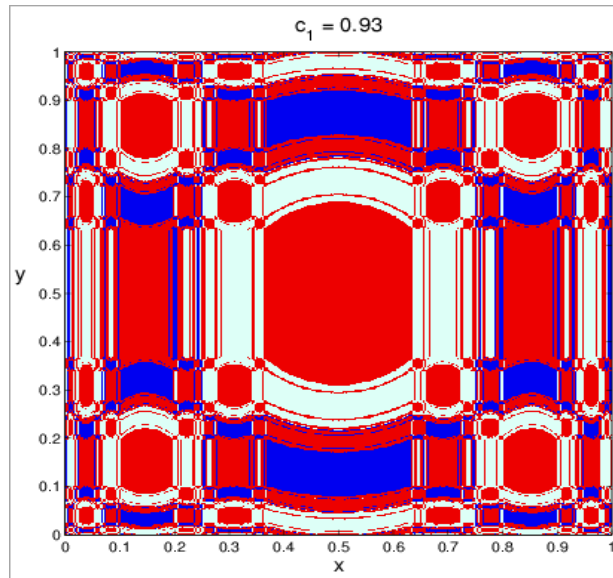

Figure 7: Basins of attraction for $N = 2$ and $c_1 = 0.93$. Here the accumulation of components of the basins appears to occur on a Cantor set even though $c_1 < \xi_2$.
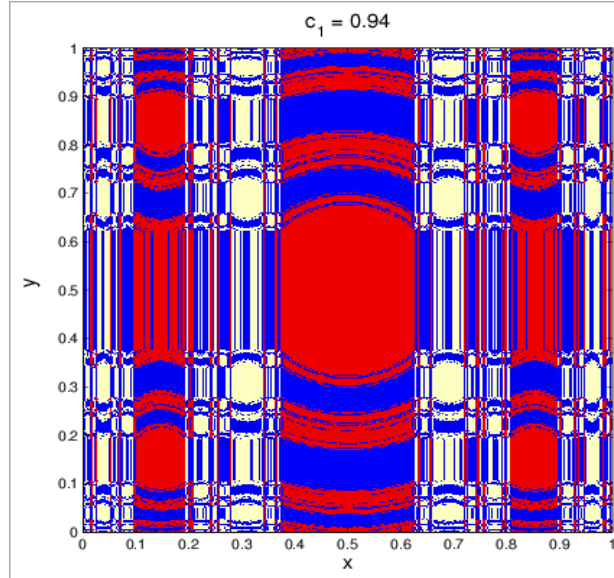
Figure 8: Basins of attraction for $N = 2$ and $c_1 = 0.94 > \xi_2$.
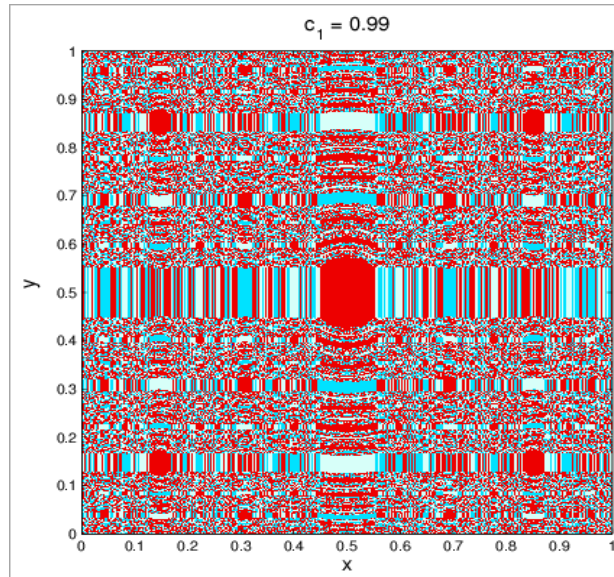

Figure 9: Basins of attraction for $N = 2$ and $c_1 = 0.99$.

c_1	Attractors	Λ	Accumulation
$.75 - .8362...$	period 2, in-phase	$\{3/4\}^N$	N/A
$.8362 - .9045...$	in-phase and ripple: 2^{N-1}	$\{3/4\}^N$	at corners
$.9045... - .9330...$	various*	expanding	in interior*
$.9330... - .9375$	various*	Cantor set	at Λ
$.9375... - 1.0$	in-phase and ripple: p^{N-1}	Cantor set	at Λ

Table 2: Summary of dynamics for cascading systems. An * indicates observations from numerics. All others are from proofs.

extends in the y direction. This is easily explained by the cascading. For initial points with x close to 0.5 and y close to C, the cascading pushes the next value of y above the threshold. In higher dimensions this effect will be more pronounced. In fact we have the following:

Proposition 4.1 *Suppose that for some $j < N$ we have $j(1 - c_1) > 1$, then the central component of in-phase locking will extend to the boundary of $[0, 1]^N$.*

Without cascading, the basins of attraction would be cross-products of inverse images of C, i.e. they would be rectangular boxes in $[0, 1]$. The cascading effective perturbs the shape of these basins in the variable after the first. The further along the array, the greater the potential perturbation.

A summary of our results and numerical observations is contained in Table 4 We have established that cascading maps have multiple basins for a relatively large range of threshold values. We have shown that if a cascading system has multiple basins then those basins have infinitely many components which accumulate at the boundary and perhaps also at points in the interior. For threshold values above $\xi_2 = \frac{2+\sqrt{3}}{4} \approx 0.933012702$ this can be very complicated since it can occur at all points in an Cantor set.

The observations suggests that these maps do not seem promising for applications in pattern recognition, since one has no hope of approximating an arbitrarily shaped set by one of the basins of attraction. However, trials using these maps to classify real medical data have been successful [Par02]. Explanations of this need to be investigated.

References

[ASY97] K. Alligood, T. Sauer, J. Yorke, *Chaos: An Introduction to Dynamical Systems*, Springer-Verlag, New York, 1997.

[KatHas95] A. Katok, B. Hasselblatt, *Introduction to the Modern Theory of Dynamical Systems*, Cambridge University Press, 1995.

[HomYou02] A.J. Homburg, T. Young, Intermittency in families of unimodal maps, *Ergod. Th. Dyn. Sys.* **22** (2002), 203-225.

[Kap76] M.V. Kapronov, Cascade phase-locked loops, (Russian), *Dinamika Sistem* **11**, 76-85, 1976.

[KMS99] M. Korzinova, V. Matrosov, V. Shalfeev, Communications using cascade coupled phase-locked loop chaos. *Intl. J. Bifur. Chaos* **9** (1999), 963-973.

[MelStr93] W. de Melo, S. van Strien, *One-dimensional dynamics*, Springer-Verlag, 1993.

[MilThu88] J. Milnor, W. Thurston, On iterated maps of the interval, *Dynamical Systems: Proc. Univ. of Maryland 1986-87* LNM **1342** Springer, Berlin, New York, 465-563.

[Par02] J. Parker, *Dynamics based pattern recognition for the analysis of multivariate gene expression data.* Thesis, Vanderbilt University, 2002.

[SinBis93] S. Sinha, D. Biswas, Adaptive dynamics on a chaotic lattice *Phys. Rev. Lett.* **71** (1993), 2010 - 2013.

[Sin94] S. Sinha, Unidirectional adaptive dynamics, *Phys. Rev. E* **49** (1994), 4832 - 4842.

[SinDit99] S. Sinha, Wm. Ditto, Computing with distributed chaos, *Phys. Rev. E* **60** (1999), 363 - 377.